Investigating the Influence of Solvent Quality on RAFT-mediated PISA of Sulfonate-functional Diblock Copolymer Nanoparticles

DOI:
10.1039/C9PY01912J

Document Version
Accepted author manuscript

Polymer Chemistry

Accepted Manuscript

This article can be cited before page numbers have been issued, to do this please use: S. Wen, J. G. Saunders and L. A. Fielding, *Polym. Chem.*, 2020, DOI: 10.1039/C9PY01912J.

ROYAL SOCIETY OF CHEMISTRY

rsc.li/polymers

View Article Online
DOI: 10.1039/C9PY01912J

ARTICLE

Investigating the Influence of Solvent Quality on RAFT-mediated PISA of Sulfonate-functional Diblock Copolymer Nanoparticles

Received 00th January 20xx,
Accepted 00th January 20xx

DOI: 10.1039/x0xx00000x

Shang-Pin Wen,[a] Jack G. Saunders,[a] and Lee A. Fielding*[a]

Polymerisation-induced self-assembly (PISA) has become widely recognised as a versatile and efficient strategy to prepare well-defined diblock copolymer nanoparticles in a range of solvents. In this article, we report the synthesis of anionic, sterically stabilised, sulfonate-functional diblock copolymer nanoparticles *via* PISA using a reversible addition–fragmentation chain transfer (RAFT) polymerisation formulation. Anionic poly(potassium 3-sulfopropyl methacrylate) (PKSPMA) macromolecular chain-transfer agents (macro-CTAs) were synthesised *via* RAFT solution polymerisation followed by chain-extension with benzyl methacrylate (BzMA) in alcohol/water mixtures to form PKSPMA-PBzMA nanoparticles. The influence of solvent quality on the formation of these nanoparticles was investigated by judiciously changing the alcohol/water ratio, the alcohol co-solvent (ethanol or methanol) and relative copolymer composition. The resulting diblock copolymer nanoparticles were analysed by dynamic light scattering (DLS), transmission electron microscopy (TEM), small-angle X-ray scattering (SAXS), and aqueous electrophoresis. The results demonstrated that nanoparticles with controllable diameters for a fixed copolymer composition can be prepared by altering the co-solvent composition. More specifically, when using different ratios of ethanol/water or methanol/water, the size of nanoparticles can be tuned from approximately 20 to 200 nm with fixed copolymer composition. This indicates that the solvency of both the stabiliser and core-forming block has a marked impact on both the aggregation of polymer chains during self-assembly and the resulting nanoparticles. Additionally, these nanoparticles remain colloidally stable and highly anionic over a wide pH range from 4 to 10, as judged by aqueous electrophoresis.

Introduction

Self-assembly of amphiphilic block copolymers comprising a hydrophilic and a hydrophobic block in selective solvents has attracted significant attention for decades.[1-3] They have potential applications in various fields, such as coatings,[4] sensing,[5] and drug delivery.[6] It is well-known that amphiphilic diblock copolymers self-assemble to form well-defined nanoparticles in appropriate selective solvents for one of the two blocks.[7-9] Self-assembly is typically conducted in dilute solution (<1%) using various post-polymerisation methods, such as pH switch,[10] thin film rehydration[11] or solvent exchange.[12] Principally, the nanoparticle morphology and mean diameter depends on the relative volume fractions of the solvophobic and solvophilic blocks which dictate the packing parameter.[13]

Recently, polymerisation-induced self-assembly (PISA) *via* reversible addition–fragmentation chain transfer (RAFT) polymerisation has attracted considerable interest for the design and preparation of a wide range of complex block copolymer nanoparticles with controlled size, morphology, and surface functionality.[14-16] PISA is also a versatile and efficient route to prepare a wide range of diblock copolymer nanoparticles at high solids[17] without the requirement for conventional post-polymerisation processing techniques, making this method amenable to scale-up for industrial production.[18] Furthermore, RAFT-mediated PISA can be performed in a wide range of media such as alcohols,[19-21] water,[22-24] and non-polar solvents.[25-27] Briefly, in this technique, a RAFT macromolecular chain transfer agent (macro-CTA) is utilised as a soluble stabiliser block, which is chain-extended using a solvent-miscible or a solvent-immiscible monomer *via* RAFT dispersion or emulsion polymerisation, respectively, to form a second block.

During RAFT dispersion polymerisation, a solvent-miscible monomer chain extends a soluble macro-CTA and gradually forms an insoluble block as the degree of polymerisation (DP) increases. *In situ* self-assembly occurs to form sterically stabilised nanoparticles such as spherical micelles (spheres), worm-like micelles (worms) and vesicles.[28, 29] In contrast, during RAFT emulsion polymerisation, the monomer is solvent-immiscible. Although most of the monomer is water-insoluble,

[a] *Department of Materials, School of Natural Sciences, University of Manchester, Oxford Road, Manchester, M13 9PL, U.K.*

† Electronic Supplementary Information (ESI) available: Experimental details of the synthesis and characterisation of PETTC; ^{1}H NMR spectra of $PKSPMA_{32}$; kinetic studies for the synthesis of $PKSPMA_{53}$; GPC chromatograms for $PKSPMA_x$ self-blocking experiments; Solubility of BzMA, $PKSPMA_{32}$ and $PKSPMA_{53}$; additional TEM images; SAXS scattering data and fitting parameters; tables detailing the particle diameters of the $PKSPMA_x$–$PBzMA_y$ particles reported in this study; and viscosity, refractive index, and dielectric constant values for DLS hydrodynamic diameter calculations. See DOI: 10.1039/x0xx00000x

View Article Online
DOI: 10.1039/C9PY01912J

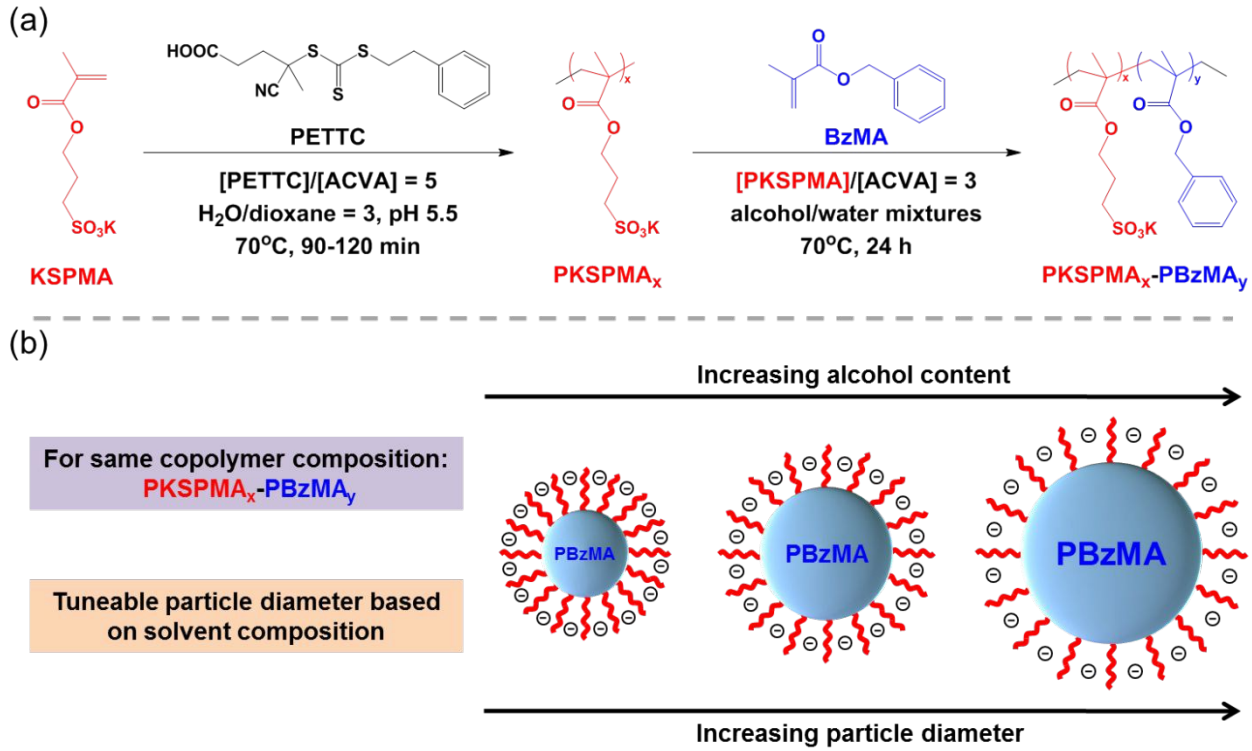

Scheme 1 (a) Synthesis of poly(potassium 3-sulfopropyl methacrylate) (PKSPMA) macro-CTA *via* RAFT solution polymerisation at 70 °C (15 % w/w, pH 5.5), followed by RAFT-mediated PISA of benzyl methacrylate (BzMA) in alcohol/water mixtures at 70 °C (10 % w/w). (b) Schematic representation of how solvent quality affects the resulting nanoparticle diameter for a fixed target PKSPMA-PBzMA composition.

monomer units to the macro-CTA, nucleation occurs, and monomer-swollen micelles are formed. Importantly, the low solvation of the growing block copolymer chains hinders the formation of higher-order nanoparticle morphologies during polymerisation and typically only kinetically trapped spheres are obtained *via* RAFT emulsion polymerisation.[14, 30, 31]

Sulfonate functional groups are frequently present in biologically important macromolecules, which can have potential antibacterial applications,[32, 33] and can be also used to modify the growth of inorganic crystals.[34] Thus the preparation of sulfonate-functional nanoparticles with tuneable sizes and controllable surface chemistries are of great interest. Sulfopropyl methacrylate potassium salt (KSPMA) is a commercially available monomer which has also been used in previous PISA formulations.[35-37] For example, Ma et al.[35] prepared PKSPMA-PBzMA diblock copolymer nanoparticles *via* RAFT aqueous emulsion polymerisation. Spherical nanoparticles with small diameters (56 nm) were obtained but DLS reported relatively high polydispersity indexes for these particles, which indicates relatively poor control over the PISA process was achieved.

Typically, either a dispersion or emulsion polymerisation formulation is used to probe the assembly of nanoparticles during PISA. This is often achieved by varying the DP of the macro-CTA or core-forming block,[38-41] by changing the copolymer concentration[38-41] or by varying the macro-CTA chemistry (e.g. using statistical copolymerisation,[26, 42] or by a 'mixed macro-CTA' approach[43, 44]). However, only a few studies have investigated the role of solvent quality during PISA[2, 45] and as far as we are aware, there are relatively few detailed investigations of PISA in the intermediate conditions between emulsion and dispersion polymerisation.

Recently, Ning et al.[46] prepared poly(ammonium 2-sulfatoethyl methacrylate)-b-poly(benzyl methacrylate) (PSEM–PBzMA) *via* RAFT aqueous emulsion polymerisation and dispersion polymerisation in a 2:1 v/v ethanol/water mixture. Spherical nanoparticles were obtained in both cases. The nanoparticles synthesised *via* RAFT dispersion polymerisation were significantly larger (80-126 nm versus 31-36 nm) and had higher mean aggregation numbers (1200-4100 versus 40-70) than those prepared *via* aqueous emulsion polymerisation.

Herein we report the preparation of amphiphilic diblock copolymer nanoparticles in alcohol/water mixtures. More specifically, a series of PKSPMA-PBzMA nanoparticles have been prepared by systematically adjusting the alcohol/water ratio of the continuous phase (Scheme 1). This has allowed us to extend the knowledge of the rules which govern nanoparticle formation during PISA. We demonstrate that nanoparticles with tuneable diameters can be synthesised by altering the co-solvent composition for a fixed stabiliser and/or core-forming block. The resulting nanoparticles were characterised *via* DLS, TEM, SAXS, and aqueous electrophoresis. Moreover, the colloidal stability and the

ability to redisperse these nanoparticles from a dried state is demonstrated. For the sake of brevity, a shorthand label is used throughout this manuscript: PKSPMA and PBzMA or "S" and "B" are utilised to denote the two blocks, respectively.

Experimental

Materials

3-Sulfopropyl methacrylate potassium salt (KSPMA, 98%) and 4,4'-azobis(4-cyanovaleric acid) (ACVA, 99%) were purchased from Sigma-Aldrich (UK) and used as received. Benzyl methacrylate (98%) was purchased from Alfa Aesar (UK) and passed through a column of activated basic alumina to remove inhibitors and impurities before use. 1,4-Dioxane was purchased from Honeywell (UK) and used as received. Deuterium oxide (D_2O) and *d*-chloroform ($CDCl_3$) used for NMR studies were purchased from Cambridge Isotope Laboratories (UK). Methanol (>99.9%) and ethanol (95%) were purchased from Fisher Scientific (UK) and used as received. 4-Cyano-4-(2-phenylethane sulfanylthiocarbonyl) sulfanylpentanoic acid (PETTC) was prepared in-house (ESI†).[36] Dialysis tubing (regenerated cellulose, MWCO = 3.5 kDa and diameter = 29 mm) was received from Fisher Scientific. Deionised water was used in all experiments.

Synthesis of poly(3-sulfopropyl methacrylate) *via* RAFT solution polymerisation

The synthesis of PKSPMA macro-CTAs has been described in detail elsewhere.[35, 36] In a typical protocol for the synthesis of $PKSPMA_{32}$, a round-bottomed flask was charged with KSPMA (15.0 g, 60.9 mmol), PETTC (689.1 mg, 2.0 mmol, dissolved in dioxane), ACVA (113.8 mg, 0.4 mmol, PETTC/ACVA molar ratio = 5), and pH 5.5 acetate buffer (66.6 g, final buffer/dioxane ratio = 3). The sealed reaction vessel was deoxygenated with nitrogen for 30 min and placed in a preheated water bath at 70 °C for 90 min. The resulting $PKSPMA_{32}$ macro-CTA (90% conversion; M_n = 7400 g mol^{-1}, M_w/M_n = 1.13) was purified by dialysis against 10:1 water/methanol and isolated under vacuum overnight. The DP for this macro-CTA was calculated using ^{1}H NMR spectroscopy (Fig. S1, ESI†) by comparing the integrated proton signals corresponding to the methacrylic polymer backbone at 0.4-2.5 ppm with those corresponding to the aromatic protons of the PETTC chain end at 7.2-7.4 ppm. $PKSPMA_{53}$ macro-CTA (polymerisation time = 120 min; 86% conversion; M_n = 9800 g mol^{-1}, M_w/M_n = 1.12) was synthesised and characterised using the same procedure.

Synthesis of PKSPMA-PBzMA diblock copolymer nanoparticles

A typical protocol for the synthesis of $PKSPMA_x$-$PBzMA_y$ (S_x-B_y) diblock copolymer nanoparticles at 10 % w/w solids in alcohol/water mixtures was as follows. For $PKSPMA_{32}$-$PBzMA_{100}$ synthesised in methanol/water, BzMA (220.2 mg, 1.220 mmol), $PKSPMA_{32}$ macro-CTA (85.2 mg, 0.012 mmol), ACVA (1.1 mg, 0.004 mmol, CTA/initiator molar ratio = 3) and methanol/water (2.7 g) were weighed into a 14 mL vial. The vial was sealed and purged with nitrogen for 10 min before being placed in a preheated oil bath at 70 °C for 24 h to ensure complete conversion of BzMA. Polymerisations were quenched by cooling to room temperature and opening to air. Monomer conversions were determined *via* gravimetry by drying approximately 0.1 g of the final dispersion at 80 °C until constant weight. In subsequent syntheses, the DP of the two blocks and the solvent was varied using methanol/water and ethanol/water mixtures, using the procedure described above. Unfortunately, GPC and NMR cannot readily be utilised to characterise S_x-B_y diblock copolymers as no suitable solvents were available due to the highly amphiphilic nature of these block copolymers. Thus, a relatively low CTA/initiator ratio of 3 was used during the synthesis of these copolymers. This ensured high BzMA conversions (>99% in all cases, as judged by gravimetry of the final reaction dispersion) and is consistent with prior literature on related PISA formulations.[46, 47]

Characterisation

Proton (^{1}H) and carbon (^{13}C) nuclear magnetic resonance spectroscopy (NMR) spectra were acquired on a Bruker Advance III 400 MHz spectrometer with 128 scans averaged per spectrum. Samples were dissolved in either D_2O or $CDCl_3$ prior to NMR analysis.

Molar mass distributions of PKSPMA were determined by aqueous gel permeation chromatography (GPC) equipped with two PL aquagel-OH MIXED-H 8 µm columns at ambient temperature. Phosphate buffer at pH 9 with 30 % v/v methanol was used as an eluent at a flow rate of 1.0 mL min^{-1}. A refractive index detector (Shodex RI-101) was used and the system was calibrated with a series of near-monodisperse poly(ethylene oxide) standards.

Transmission electron microscopy (TEM) images were recorded using a Philips CM 20 instrument operating at an accelerating voltage of 200 kV and connected to a Gatan 1k CCD camera. Samples for TEM observations were prepared by depositing 3 µL of diluted copolymer dispersion onto 400 mesh carbon-coated copper grids for 30 min and then carefully blotted with filter paper to remove excess solution. The samples were stained in the vapour space above ruthenium tetroxide (RuO_4) solution for 7 min at room temperature.[48] The mean nanoparticle diameters was determined by ImageJ software and over 200 randomly selected particles were measured for each sample.

Dynamic light scattering (DLS) studies were performed using a Malvern Zetasizer Nano ZS instrument equipped with a He–Ne solid-state laser operating at 633 nm and back-scattered light at a scattering angle of 173°. Copolymer dispersions were diluted to approximately 0.1 % w/w using the same alcohol/water mixture used during the synthesis of the particles. DLS samples were analysed at 25 °C using disposable plastic cuvettes and data were averaged over three consecutive measurements. The parameters for calculating hydrodynamic diameters (D_h) were obtained by fitting literature values of reflective index,[49] viscosity,[50] and dielectric constant[51] (Table S3, ESI†).

View Article Online DOI: 10.1039/C9PY01131

Aqueous electrophoresis studies for the diblock copolymer nanoparticles were analysed using the same Malvern Zetasizer Nano ZS instrument described above. The solution pH was initially adjusted to 10 using 0.1 M KOH in the presence of 1.0 mM KCl. The solution pH was then manually lowered from 10 to 4 using 0.01 M HCl as required. Aqueous dispersions (approximately 0.1 % w/w) were analysed at 25 °C using disposable folded capillary cell (Malvern DTS1017) and data were averaged over three consecutive measurements.

Small-angle X-ray scattering (SAXS) patterns were collected in batch mode on beamline B21 at the Diamond Light Source synchrotron facility (Didcot, UK). Data were recorded at 13.1 keV (wavelength 0.0946 nm), at a sample-detector distance of 2694.2 mm using an Eiger 4M detector. This corresponds to a scattering vector (q) range from 0.0032 to 0.38 Å^{-1}, where $q = 4\pi\sin\theta/\lambda$, where θ is a half of the scattering angle and λ is wavelength of X-ray radiation. SAXS samples were prepared using copolymer dispersions diluted with the corresponding alcohol/water mixture to 1.0 % w/w. All samples and solvents were loaded into a 96-well plate, and 30 µl of each sample was sequentially injected into a temperature-controlled quartz capillary (10 µm thick) using the BioSAXS robot (designed by the EMBL in Grenoble). The X-ray scattering data were analysed (i.e., averaged, background subtraction, data modelling and fitting) using Irena SAS macros for Igor Pro.[52] Structural parameters were determined by fitting 1D SAXS patterns using a two-population model of spherical micelles[53] plus Gaussian polymer chains[41] with related fitting parameters shown in Table S4 (ESI†). This approach enabled the determination of structural parameters for the nanoparticles, such as the radius of gyration of the stabiliser chains (R_g), mean radius of core (R_{core}), solvent fraction in the core (X_{sol}), and mean aggregation number (N_{agg}).

Results and discussion

Synthesis of PKSPMA macro-CTAs

RAFT solution polymerisation of KSPMA was conducted in 3:1 water/dioxane at 70 °C (Scheme 1). Fig. 1a shows conversion and semi-logarithmic kinetics versus reaction time for $PKSPMA_{32}$. About 90% conversion was achieved within 90 min. The approximately linear relationship between $\ln([M]_0/[M])$ and reaction time indicated the polymerisation was first-order with respect to monomer concentration.[26] It is noteworthy that all GPC chromatograms of samples taken during the preparation of $PKSPMA_{32}$ and $PKSPMA_{53}$ were unimodal and successively shifted to shorter retention times (Fig. 1c and Fig. S2c, ESI†).

The evolution of molar mass and molar mass dispersity (M_w/M_n) versus monomer conversion for $PKSPMA_{32}$ are shown in Fig. 1b. As the polymerisation progressed, the corresponding dispersity declined, and the resulting macro-CTA had a relatively narrow molar mass distribution (M_w/M_n = 1.13) at 90% conversion. Moreover, the blocking efficiency of the PKSPMA macro-CTAs were examined by self-blocking experiments (Fig. S3, ESI†). Briefly, addition of a further charge of KSPMA (target DP 300) lead to chain extension. GPC analysis of the resulting chain-extended homopolymer confirmed unimodal distributions and relatively low molar mass dispersities (~1.26) in both cases. This that these macro-CTAs are likely undergo efficient chain extension to form second blocks with other monomers, as desired.[47, 54]

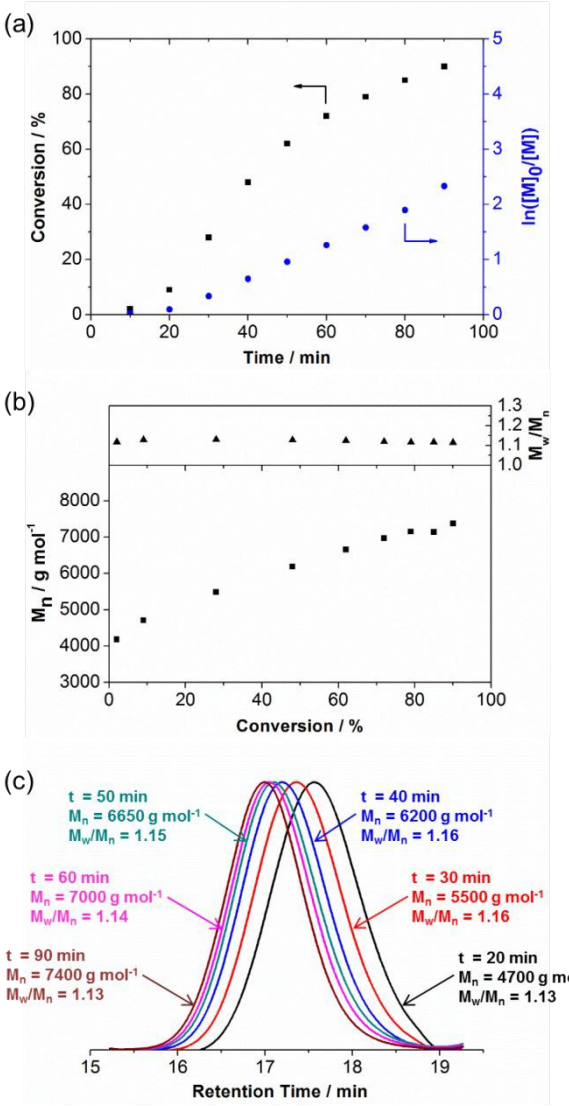

Fig. 1 Kinetic studies for RAFT solution polymerisation of KSPMA (target DP 30) with PETTC as a CTA in 3:1 water/dioxane at 70 °C: (a) conversion and semi-logarithmic kinetics versus reaction time, (b) M_w/M_n and M_n versus monomer conversion, and (c) aqueous GPC chromatograms. Preparation of PKSPMA-PBzMA nanoparticles in various alcohol/water mixtures.

Sulfonate-functional nanoparticles were prepared *via* RAFT-mediated PISA in various alcohol/water mixtures. The synthesis of related anionic sterically stabilised nanoparticles have been conducted *via* RAFT aqueous emulsion polymerisation[35] or RAFT alcoholic dispersion polymerisation.[20] In this work, the core-forming monomer, BzMA, is soluble in alcohol-rich solvent compositions whereas the PKSPMA stabiliser is soluble in water-rich solvent mixtures (Fig. S4, ESI†). For example, BzMA dissolves at ethanol contents >70 % w/w but visible phase separation occurs at water contents >30

% w/w. In contrast, PKSPMA cannot dissolve when the ethanol content is higher than approximately 70 % w/w (or ~85 % w/w for methanol/water mixtures). Importantly, PBzMA is insoluble in all solvent combinations reported herein.[55] Thus, in this work, we have investigated PISA at intermediate solvent compositions between wholly aqueous emulsion and alcoholic dispersion polymerisation conditions. $PKSPMA_x$–$PBzMA_y$ nanoparticles were therefore prepared under various intermediate

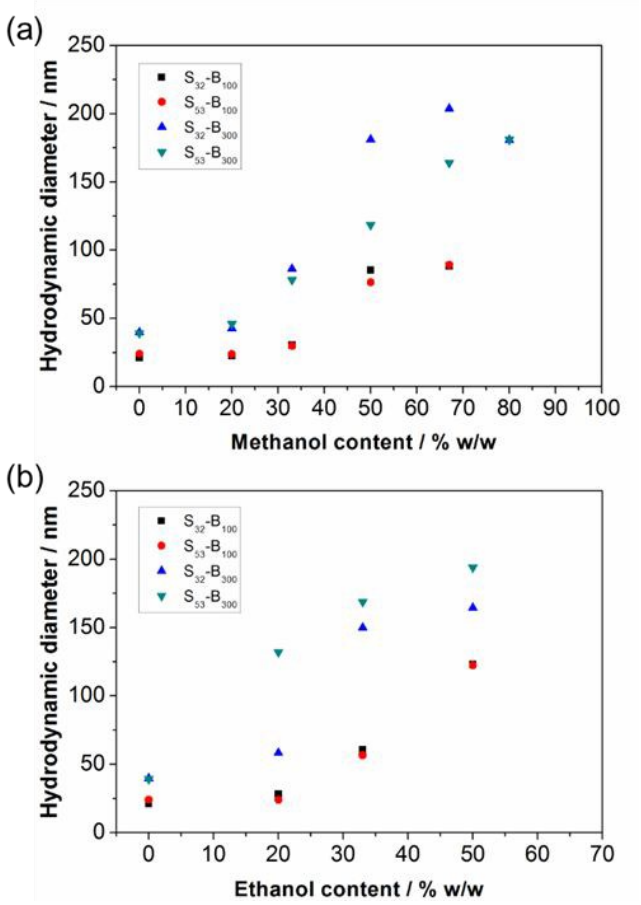

Fig. 2 Mean hydrodynamic diameters of S_x-B_y diblock copolymer nanoparticles synthesised in varying (a) methanol/water and (b) ethanol/water mixtures at 10% w/w solids and 70 °C.

alcohol/water mixtures as a mechanism of probing the effect of solvent quality on the particle diameter, morphology, and composition of the resulting nanoparticles (Scheme 1, Table S1 and Table S2, ESI†).

Fig. 2 shows mean hydrodynamic diameters of S_x-B_y particles synthesised in methanol/water and ethanol/water mixtures. In Fig. 2a, the mean particle diameters became larger as the methanol content increased. For example, in the S_{32}-B_{300} series, the mean hydrodynamic diameter increased five-fold, from approximately 40 to 200 nm for methanol contents in the range 0 to 67 % w/w. On increasing the methanol content to 80 % w/w, the mean particle diameter determined by DLS decreased to 181 nm, whereas the mean diameter calculated from TEM image analysis was 194 nm. This discrepancy is likely due to the PKSPMA stabiliser being close to its solubility limit (Fig. S4, ESI†). When DLS analysis was conducted on particles transferred to wholly aqueous media, the mean particle diameter was determined to be 197 nm, indicating better solvation of the PKSPMA corona. This observation was consistent across all particles studied (Table S1, ESI†). Furthermore, the change in particle diameter for a fixed copolymer composition suggests that solvent quality dramatically affects the PISA process.[56] For instance, in a water rich solvent mixture, the hydrophilic PKSPMA block can stretch easily, but the PBzMA block is constrained significantly due to the high hydrophobicity of PBzMA. This constraint at higher water contents results in the observed smaller particle

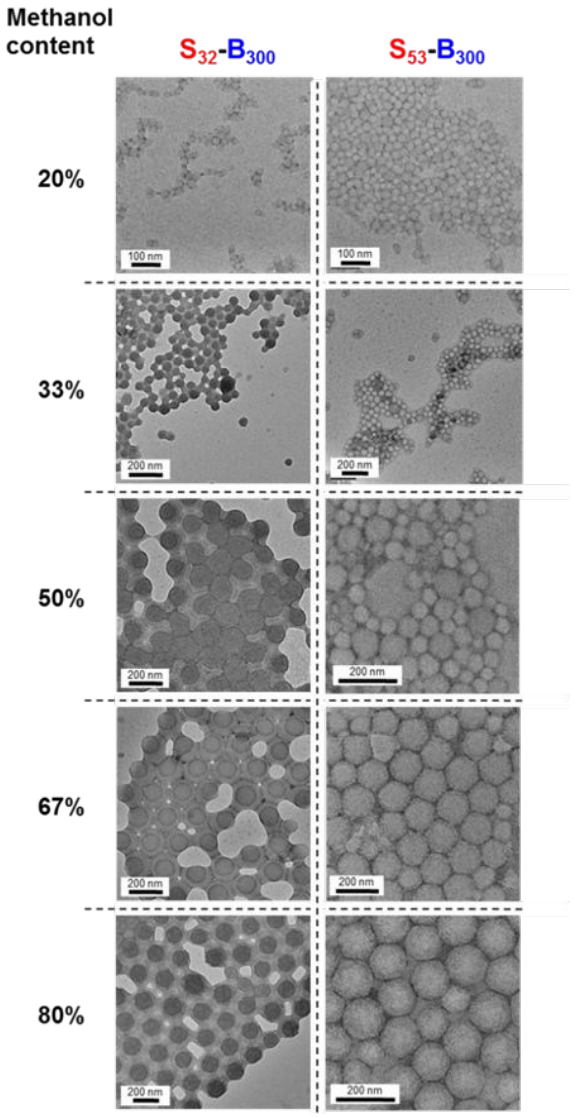

Fig. 3 Representative TEM images of S_{32}–B_{300} and S_{53}–B_{300} diblock copolymer nanoparticles prepared at 10 % w/w solids *via* RAFT-mediated PISA in methanol/water mixtures at 70 °C.

diameters as the copolymer chains are not solvated and unable to exchange.[57] In contrast, the PBzMA block will be more swollen and thus occupy more volume during PISA at higher alcohol/water ratios, resulting in the larger particle diameters observed. At methanol contents >67-80 % w/w, phase separation occurred and no colloidally stable particles were present in the final dispersion. For ethanol/water mixtures (Fig. 2b) a similar trend was observed as for methanol/water, i.e. with increasing ethanol content the mean hydrodynamic diameter increased up to an ethanol content of

50 % w/w. However, phase separation occurred with ethanol contents higher than 67 % w/w. This correlates with the solubility of PKSPMA homopolymer which is soluble in alcohol/water mixtures up to ~70 % w/w ethanol or ~85 % w/w methanol (Fig. S4, ESI†). Thus, at higher ethanol contents, this highly anionic macro-CTA can no longer stabilise the nanoparticles and precipitation occurs during polymerisation.

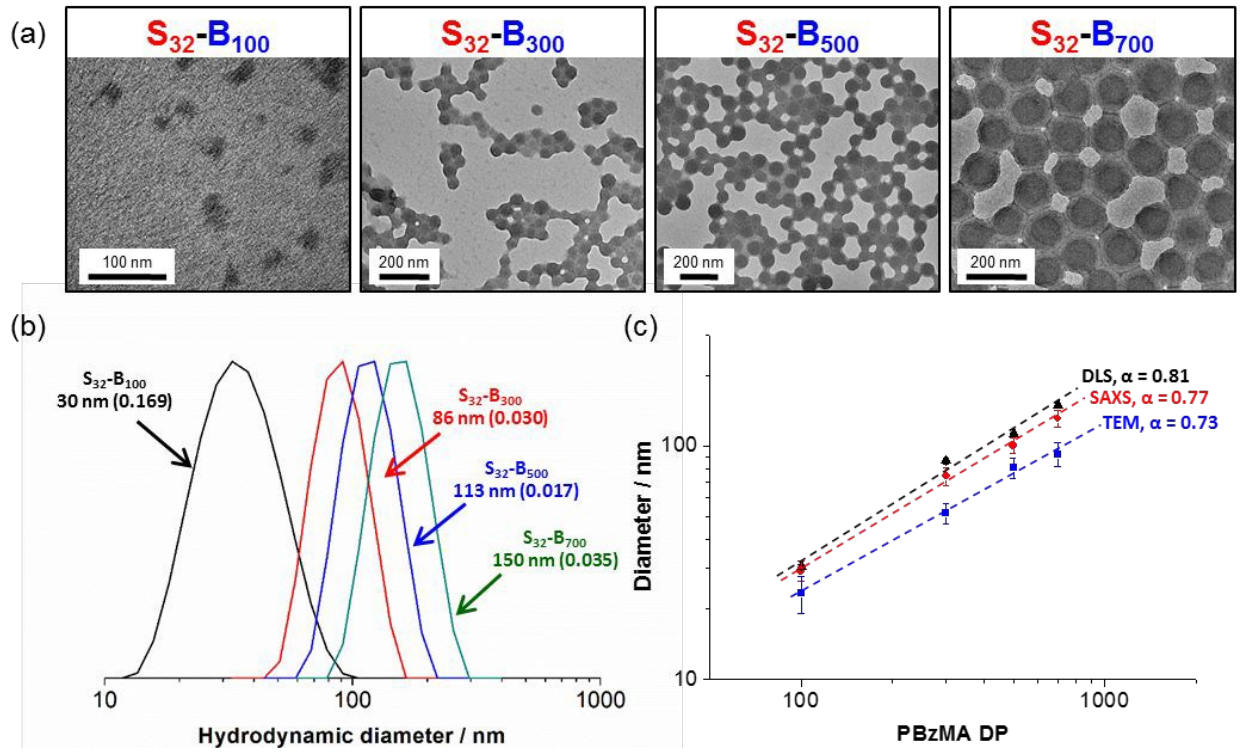

Fig. 4 $S_{32}-B_x$ diblock copolymers nanoparticles prepared at 10 % w/w solids *via* RAFT-mediated polymerisation of BzMA in methanol/water mixture at 33 % w/w methanol content. (a) TEM images of $S_{32}-B_y$ (y = 100, 300, 500, and 700), (b) corresponding DLS intensity-average size distributions (the number in brackets represents the DLS polydispersity index), and (c) mean particle diameter versus degree of polymerisation of the PBzMA core-forming block.

The morphologies of the S_x-B_y diblock copolymer nanoparticles prepared at various methanol/water (Fig. 3) and ethanol/water (Fig. S5) ratios were investigated *via* TEM after staining with RuO_4. This stain highlights the aromatic PBzMA block[58] in these particles hence some of the images appear to have a distinct core-shell morphology. In all cases spherical micelles were obtained, with diameters generally in agreement with DLS (Fig. 2, Table S1, and Table S2, ESI†). This observation agrees with previous studies, which also only obtained spheres for PKSPMA-PBzMA[35] and PSEM-PBzMA[46] PISA formulations. This is likely due to the highly anionic character of PKSPMA preventing higher order morphology formation.

Preparation of S_x-B_y nanoparticles with varying PBzMA DP

The mean diameters of S_x-B_y nanoparticles can also be tuned by simply altering the DP of PBzMA. Specifically, for a fixed $PKSPMA_{32}$ macro-CTA, a monotonic increase in mean hydrodynamic diameter was observed when increasing the DP of PBzMA from 100 to 700 (Fig. 4). For instance, the mean hydrodynamic diameter of $S_{32}-B_{100}$ was 30 nm, while $S_{32}-B_{700}$ formed nanoparticles with diameters of 150 nm. The spherical morphology and particle diameters reported by DLS (Fig. 4b) and SAXS (Table 1) were also verified by TEM images (Fig. 4a). DLS particle size distributions remained relatively narrow for nanoparticles with PBzMA DPs >100, even when targeting highly asymmetric core-forming block compositions, such as $S_{32}-B_{700}$. It is worth noting that whilst the S_{32}-B_{100} particles were very difficult to image *via* TEM (Fig. 4a), both DLS and SAXS data support that the objects observed are spherical nanoparticles.

The mean spherical diameter (D) can be related to the DP of the core-forming block (y) by a scaling exponent (α), as described by the equation $D=ky^{\alpha}$, where k is a constant.[59, 60] Fig. 4c shows a double-logarithmic plot of D against y for $S_{32}-B_y$ nanoparticles prepared at 33 % w/w methanol. In all cases, a linear relationship is evident, with determined values of α of 0.81, 0.77, and 0.73 for DLS, SAXS (see section below), and TEM analysis, respectively. These high α values (> 2/3) suggest strong copolymer segregation and that the PBzMA chains are in a relatively stretched configuration.[59-61]

SAXS analysis of PKSPMA–PBzMA diblock copolymer nanoparticles

SAXS data were recorded for S_x-B_y nanoparticles and the resulting scattering patterns modelled using a spherical micelles[53] plus Gaussian polymer chains[41] model (Table S4, ESI†). From these SAXS patterns (Fig. 5 and Fig. S6, ESI†), it was possible to determine the mean radius of the micelle core (R_{core}), radius of gyration of the PKSPMA stabiliser chains (R_g), average solvent fraction in the core (X_{sol}), mean aggregation number (N_{agg}), average number of copolymer chains per unit surface area (S_{agg}), and the volume fraction of the two populations. The mean particle diameters were calculated by SAXS fitting ($D_{SAXS} = 2R_{core} + 4R_g$) and are consistent with both DLS and TEM data (Table 1, Tables S1 and S2, ESI†).

In all cases the second population, representing dissolved polymer chains, had negligible volume fractions on fitting. This resulted in fits that were not particularly sensitive to the R_g of these dissolved chains. Nevertheless, this population was included for constancy with previously published data[62] and the fitted R_g values were in the range 3 to 10 Å. This indicates that the low concentration of these dissolved chains is PKSPMA homopolymer (calculated R_g of 14.4 and 18.6 Å for DP 32 and 53, respectively), rather than S_x-B_y copolymer chains.

Table 1 Summary of mean particle diameters and SAXS structural parameters for S_x-B_y nanoparticles prepared in different alcohol/water mixtures.

Entry	Target Composition	Dispersant	Alcohol content / % w/w	Particle diameter (nm)			Structural parameters					
				D_{DLS}[a]	D_{TEM}[b]	D_{SAXS}[c]	R_{core}[d] (Å)	σR_{core}[e] (Å)	R_g[f] (Å)	X_{sol}[g]	N_{agg}[h]	S_{agg}[i]
1	S_{32}-B_{300}	methanol/water	20	42 ± 0	25 ± 2	40 ± 5	138	26	31.5	0.00	147	0.062
2	S_{32}-B_{300}	methanol/water	33	86 ± 2	52 ± 5	74 ± 6	313	32	28.8	0.17	1430	0.116
3	S_{32}-B_{300}	methanol/water	50	181 ± 3	147 ± 14	161 ± 9	774	44	15.5	0.17	21777	0.289
4	S_{32}-B_{300}	methanol/water	67	204 ± 2	159 ± 12	179 ± 8	849	39	22.9	0.44	19119	0.211
5	S_{32}-B_{100}	methanol/water	33	30 ± 0	23 ± 4	29 ± 3	92	14	27.1	0.07	125	0.116
6	S_{32}-B_{500}	methanol/water	33	113 ± 2	81 ± 8	101 ± 8	455	41	24.4	0.21	2519	0.097
7	S_{32}-B_{700}	methanol/water	33	150 ± 1	92 ± 11	131 ± 11	636	57	9.3	0.34	4081	0.080
8	S_{32}-B_{300}	ethanol/water	33	150 ± 2	101 ± 8	132 ± 7	613	35	22.7	0.02	12762	0.270

[a] Mean hydrodynamic diameter obtained *via* DLS analysis. [b] Mean TEM particle diameters were calculated by analysing 200 particles using ImageJ software. [c] SAXS diameters were calculated using $D_{SAXS} = 2R_{core} + 4R_g$. [d] R_{core} represents mean radius of the spherical core. [e] σR_{core} represents standard deviation of the core radius. [f] R_g represents radius of gyration of the PKSPMA stabiliser. [g] X_{sol} represents solvent fraction in the micelle core. [h] N_{agg} represents mean aggregation number and is calculated using Equation 1. [i] S_{agg} represents average number of copolymer chains per unit surface area and is calculated using Equation 2.

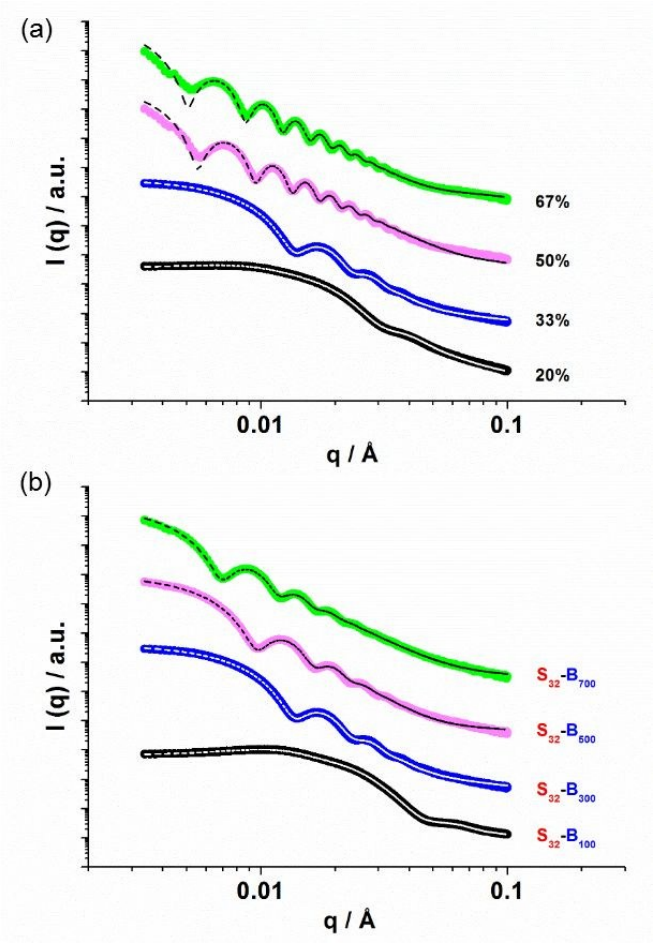

Fig. 5 Selected small-angle X-ray scattering data (coloured circles) recorded for 1.0 % w/w copolymer dispersions for nanoparticles prepared at 10 % w/w solids *via* RAFT-mediated PISA of (a) S_{32}–B_{300} synthesised at various methanol contents (indicated on Figure), and (b) S_{32}–$B_{100\text{-}700}$ nanoparticles prepared in 33 % w/w methanol/water mixtures. Dashed lines represent fits to the data using a spherical micelles[52] plus Gaussian polymer chains[41] model.

The SAXS fitting parameters of S_x-B_y nanoparticles prepared in different methanol/water mixtures are shown in Table 1 (Entries 1-4). As the alcohol content is increased, R_g of the PKSPMA stabiliser block slightly decreases. This is presumably because at higher methanol contents, the solvent has a lower polarity, resulting in the shrinkage of the highly hydrophilic PKSPMA chains. As the methanol content is increased, the particle diameter becomes significantly larger. This is consistent with DLS (Fig. 2) and TEM (Fig. 3). As the alcohol content increases from 20 to 67 % w/w, X_{sol} increases significantly from 0 to 0.44. This indicates that methanol occupies more volume in the micelle cores at higher alcohol contents during the PISA process. Thus, the core-forming PBzMA chains are swollen and consequently larger particle diameters are obtained.

The structural parameters of S_x-B_y nanoparticles can also be tuned by altering the DP of the PBzMA block (Table 1, Entries 2 and 5-7). Specifically, for a fixed S_{32} stabiliser block for particles synthesised at 33 % w/w methanol content, a monotonic increase in particle diameter was observed while the targeting PBzMA DPs up to 700. This observation is consistent with DLS and TEM data discussed earlier (Fig. 4).

The number of polymeric chains present in a micelle can be represented by the mean aggregation number (N_{agg}).[63, 64] For the S_x-B_y particles reported herein, there are significant variations in the solvent fraction (X_{sol}) within the particle cores

(Table 1). We have therefore taken this into account when calculating N_{agg}, using Equation 1 (where V_{co} is the calculated volume of a PBzMA chain).

$$N_{agg} = \frac{\frac{4}{3}\pi {R_{core}}^3}{V_{co}} \times (1 - X_{sol}) \quad (1)$$

From the modelled SAXS structural parameters for the series prepared in 33 % w/w methanol/water, N_{agg} increases from 125 for S_{32}-B_{100} to 4081 for S_{32}-B_{700} (33-fold). This indicates that the average number of PBzMA chains present in a particle

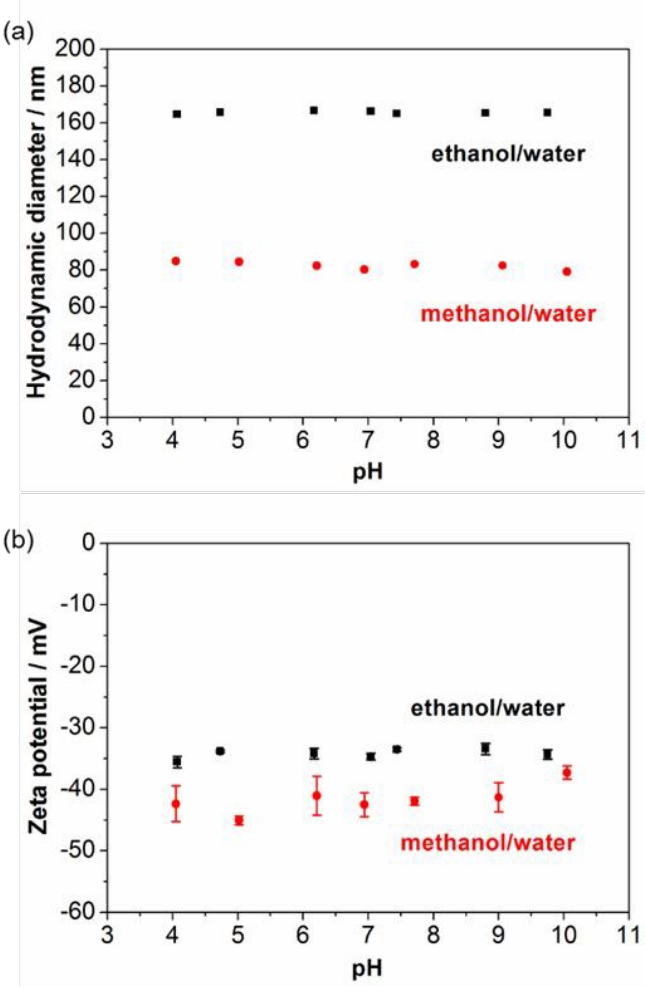

Fig. 6 Representative (a) dynamic light scattering and (b) aqueous electrophoresis data as a function of pH obtained for S_{32}-B_{300} diblock copolymer nanoparticles prepared in ethanol/water (black squares) and methanol/water (red circles) at an alcohol content of 33 % w/w. Measurements were conducted at a copolymer concentration of approximately 0.1 % w/w in the presence of 1 mM KCl as a background electrolyte

is significantly larger when targeting a higher DP. Furthermore, as both R_{core} and N_{agg} increase when targeting higher DPs of the core-forming PBzMA block (Table 1, Entries 2 and 5-7), it is pertinent to calculate the average number of copolymer chains per unit surface area (S_{agg}, Equation 2).[64]

$$S_{agg} = \frac{N_{agg}}{4\pi {R_{core}}^2} \quad (2)$$

The calculated S_{agg} values for the series prepared in 33 % w/w methanol decreased from 0.116 nm^{-2} for S_{32}–B_{100} to 0.080 nm^{-2} when targeting PBzMA DP of 700. This indicates that the surface density of the hydrophilic PKSPMA stabiliser chains becomes much lower when targeting a higher core DP. At low copolymer chain densities, the relatively hydrophobic methanol molecules can solvate the core-forming block more readily (higher X_{sol}) and thus the core occupies more volume (higher R_{core}).

For a fixed S_{32}-B_{300} copolymer composition and 33 % w/w alcohol content (Table 1, Entries 2 and 8), nanoparticles prepared in ethanol/water have significantly larger mean diameters and aggregation numbers than those obtained in

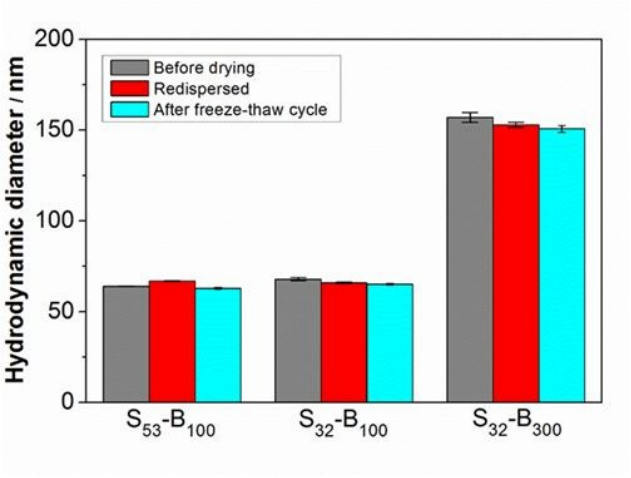

Fig. 7 Representative hydrodynamic diameters of S_x-B_y diblock copolymer nanoparticles synthesised at an ethanol content of 33 % w/w. Grey, red and blue bars represent diluted dispersions before drying; nanoparticles dried and redispersed in water; and after a freeze-thaw cycle, respectively.

methanol/water mixtures. This is presumably because the dielectric constant of a 33 % w/w ethanol/water mixture is lower than that of a 33 % w/w methanol/water mixture (Table S3, ESI†).[51] The relatively low dielectric constant of the ethanol/water mixture reduces the repulsive interactions between neighbouring anionic PKSPMA stabiliser chains during PISA, allowing more copolymer chains to assemble per unit surface area (S_{agg} in Table 1).[46, 65] Hence X_{sol} is lower for particles prepared in ethanol/water than for methanol/water mixtures. Copolymer chains will therefore be more stretched and assemble in a more compact manner.[66] This results in a higher number of copolymer chains present for particles prepared in ethanol/water mixtures and consequently larger mean diameters.[46]

Colloidal stability of PKSPMA-PBzMA nanoparticles

Fig. 6 shows DLS and aqueous electrophoresis data for S_{32}-B_{300} diblock copolymer nanoparticles, synthesised in either 33 % w/w methanol/water or 33 % w/w ethanol/water mixtures as a function of pH. According to Fig. 6a, the mean hydrodynamic diameter of the nanoparticles is independent of the solution pH, which indicates good colloidal stability over a wide pH range from 4 to 10.[47] This is clearly different from related poly(methacrylic acid) (PMAA) stabilised diblock copolymer nanoparticles where the PMAA is a weak polyelectrolyte which can be protonated and result in particle aggregation at low pH.[47, 67]

Fig. 6b shows that S_x-B_y diblock copolymer nanoparticles are highly anionic and pH-independent zeta potentials were observed, even at relatively low pH. This pH-independent character confirms that PKSPMA is present within the coronas of the particles. This strong anionic polyelectrolyte stabiliser enables flocculation to be prevented during attempted aggregation by variation of the solution pH.[36, 44, 47] As previously stated, the strong anionic nature of this stabiliser provides electrostatic repulsion between block copolymer nanoparticles during PISA and prevents the formation of worm, vesicle, or other higher order morphologies.[2]

To further demonstrate the stability of these nanoparticles, mean hydrodynamic diameters of these particles were measured after: i) drying under vacuum and redispersion in water with gentle shaking and; ii) storage at -20 °C and subsequent thawing to ambient temperature (Fig. 7). Only negligible changes in mean hydrodynamic diameter were observed in all cases. This suggests that these S_x-B_y nanoparticles can be used in subsequent studies as a dried powder. This means that they are easy and convenient to weigh precisely, and the influence of residual solvent can also be minimised. This property is especially significant for further bio-related or industrial applications of these copolymer nanoparticles.

Conclusions

RAFT solution polymerisation affords sulfonate-functional macro-CTAs which are subsequently used to prepare sulfonate-bearing spherical nanoparticles *via* RAFT-mediated PISA in alcohol/water mixtures. Nanoparticles with tuneable diameters can be prepared *via* varying the DP of the stabiliser and/or core-forming block, or by simply altering the co-solvent composition for a fixed target copolymer. This indicates that the solvency of both the stabiliser and core-forming block has a marked impact on both the aggregation of polymer chains during self-assembly and the resulting copolymer nanoparticle morphology. This approach is highly versatile and provides the ability to obtain preferred particle diameters with different copolymer compositions, or to prepare a desired copolymer composition with various particle sizes. In addition, these results demonstrate that solvency of both the stabiliser (PKSPMA) and core-forming block (PBzMA) have a marked impact on both the aggregation of polymer chains during self-assembly and the resulting copolymer nanoparticle morphology. Furthermore, the ability of these highly anionic particles to be easily redispersed after drying is promising for application in future studies.

Conflicts of interest

There are no conflicts to declare.

Acknowledgements

National Chung-Shan Institute of Science and Technology (NCSIST) is thanked for funding a PhD studentship for SPW. The authors thank Nikul Khunti at beamline B21 at the Diamond Light Source (Didcot, UK) for SAXS data acquisition.

Notes and references

1. L. Zhang and A. Eisenberg, *Science*, 1995, **268**, 1728-1731.
2. Y. Mai and A. Eisenberg, *Chem. Soc. Rev.*, 2012, **41**, 5969-5985.
3. S. L. Canning, G. N. Smith and S. P. Armes, *Macromolecules*, 2016, **49**, 1985-2001.
4. F. Ouhib, A. Dirani, A. Aqil, K. Glinel, B. Nysten, A. M. Jonas, C. Jerôme and C. Detrembleur, *Polymer Chemistry*, 2016, **7**, 3998-4003.
5. C. Fong, T. Le and C. J. Drummond, *Chem. Soc. Rev.*, 2012, **41**, 1297-1322.
6. B. Karagoz, L. Esser, H. T. Duong, J. S. Basuki, C. Boyer and T. P. Davis, *Polymer Chemistry*, 2014, **5**, 350-355.
7. S. Jain and F. S. Bates, *Science*, 2003, **300**, 460-464.
8. A. Blanazs, S. P. Armes and A. J. Ryan, *Macromol. Rapid Commun.*, 2009, **30**, 267-277.
9. R. K. O'Reilly, C. J. Hawker and K. L. Wooley, *Chem. Soc. Rev.*, 2006, **35**, 1068-1083.
10. R. T. Pearson, N. J. Warren, A. L. Lewis, S. P. Armes and G. Battaglia, *Macromolecules*, 2013, **46**, 1400-1407.
11. J. R. Howse, R. A. Jones, G. Battaglia, R. E. Ducker, G. J. Leggett and A. J. Ryan, *Nature materials*, 2009, **8**, 507.
12. V. Bütün, S. Armes and N. Billingham, *Polymer*, 2001, **42**, 5993-6008.
13. M. Antonietti and S. Förster, *Adv. Mater.*, 2003, **15**, 1323-1333.
14. B. Charleux, G. Delaittre, J. Rieger and F. D'Agosto, *Macromolecules*, 2012, **45**, 6753-6765.
15. M. J. Derry, L. A. Fielding and S. P. Armes, *Prog. Polym. Sci.*, 2016, **52**, 1-18.
16. N. J. Warren and S. P. Armes, *J. Am. Chem. Soc.*, 2014, **136**, 10174-10185.
17. X. Zhang, S. Boisse, W. Zhang, P. Beaunier, F. D'Agosto, J. Rieger and B. Charleux, *Macromolecules*, 2011, **44**, 4149-4158.
18. M. J. Derry, L. A. Fielding and S. P. Armes, *Polymer Chemistry*, 2015, **6**, 3054-3062.
19. W. Cai, W. Wan, C. Hong, C. Huang and C. Pan, *Soft Matter*, 2010, **6**, 5554-5561.
20. M. Semsarilar, E. R. Jones, A. Blanazs and S. P. Armes, *Adv. Mater.*, 2012, **24**, 3378-3382.
21. M. Semsarilar, E. R. Jones and S. P. Armes, *Polymer Chemistry*, 2014, **5**, 195-203.
22. J. Rieger, C. Grazon, B. Charleux, D. Alaimo and C. Jérôme, *J. Polym. Sci., Part A: Polym. Chem.*, 2009, **47**, 2373-2390.
23. S. Sugihara, A. Blanazs, S. P. Armes, A. J. Ryan and A. L. Lewis, *J. Am. Chem. Soc.*, 2011, **133**, 15707-15713.
24. A. Blanazs, A. Ryan and S. Armes, *Macromolecules*, 2012, **45**, 5099-5107.
25. L. Houillot, C. Bui, M. Save, B. Charleux, C. Farcet, C. Moire, J.-A. Raust and I. Rodriguez, *Macromolecules*, 2007, **40**, 6500-6509.
26. L. A. Fielding, M. J. Derry, V. Ladmiral, J. Rosselgong, A. M. Rodrigues, L. P. Ratcliffe, S. Sugihara and S. P. Armes, *Chemical Science*, 2013, **4**, 2081-2087.
27. L. A. Fielding, J. A. Lane, M. J. Derry, O. O. Mykhaylyk and S. P. Armes, *J. Am. Chem. Soc.*, 2014, **136**, 5790-5798.
28. J. Rieger, *Macromol. Rapid Commun.*, 2015, **36**, 1458-1471.

29. E. Chernikova, E. Lysenko, N. Serkhacheva and N. Prokopov, *Polymer Science, Series C*, 2018, **60**, 192-218.
30. M. Manguian, M. Save and B. Charleux, *Macromol. Rapid Commun.*, 2006, **27**, 399-404.
31. J. Zhou, H. Yao and J. Ma, *Polymer Chemistry*, 2018, **9**, 2532-2561.
32. V. Cagno, P. Andreozzi, M. D'Alicarnasso, P. J. Silva, M. Mueller, M. Galloux, R. Le Goffic, S. T. Jones, M. Vallino and J. Hodek, *Nature materials*, 2018, **17**, 195.
33. M. Ramstedt, N. Cheng, O. Azzaroni, D. Mossialos, H. J. Mathieu and W. T. Huck, *Langmuir*, 2007, **23**, 3314-3321.
34. C. T. Hendley IV, L. A. Fielding, E. R. Jones, A. J. Ryan, S. P. Armes and L. A. Estroff, *J. Am. Chem. Soc.*, 2018, **140**, 7936-7945.
35. J. Ma, H. M. Andriambololona, D. Quemener and M. Semsarilar, *J. Membr. Sci.*, 2018, **548**, 42-49.
36. M. Semsarilar, V. Ladmiral, A. Blanazs and S. Armes, *Langmuir*, 2011, **28**, 914-922.
37. Y. Ning, L. Han, M. J. Derry, F. C. Meldrum and S. P. Armes, *J. Am. Chem. Soc.*, 2019, **141**, 2557-2567.
38. Z. Ding, C. Gao, S. Wang, H. Liu and W. Zhang, *Polymer Chemistry*, 2015, **6**, 8003-8011.
39. J. Tan, J. He, X. Li, Q. Xu, C. Huang, D. Liu and L. Zhang, *Polymer Chemistry*, 2017, **8**, 6853-6864.
40. V. J. Cunningham, A. M. Alswieleh, K. L. Thompson, M. Williams, G. J. Leggett, S. P. Armes and O. M. Musa, *Macromolecules*, 2014, **47**, 5613-5623.
41. B. Akpinar, L. A. Fielding, V. J. Cunningham, Y. Ning, O. O. Mykhaylyk, P. W. Fowler and S. P. Armes, *Macromolecules*, 2016, **49**, 5160-5171.
42. Y.-Y. Kim, L. A. Fielding, A. N. Kulak, O. Nahi, W. Mercer, E. R. Jones, S. P. Armes and F. C. Meldrum, *Chem. Mater.*, 2018, **30**, 7091-7099.
43. C. Gonzato, M. Semsarilar, E. R. Jones, F. Li, G. J. Krooshof, P. Wyman, O. O. Mykhaylyk, R. Tuinier and S. P. Armes, *J. Am. Chem. Soc.*, 2014, **136**, 11100-11106.
44. M. Semsarilar, V. Ladmiral, A. Blanazs and S. Armes, *Langmuir*, 2012, **29**, 7416-7424.
45. L. Zhang and A. Eisenberg, *Macromolecules*, 1996, **29**, 8805-8815.
46. Y. Ning, L. A. Fielding, L. P. Ratcliffe, Y.-W. Wang, F. C. Meldrum and S. P. Armes, *J. Am. Chem. Soc.*, 2016, **138**, 11734-11742.
47. Y. Ning, L. Fielding, T. Andrews, D. Growney and S. Armes, *Nanoscale*, 2015, **7**, 6691-6702.
48. L. A. Fielding, J. A. Lane, M. J. Derry, O. O. Mykhaylyk and S. P. Armes, *J Am Chem Soc*, 2014, **136**, 5790-5798.
49. J. V. Herráez and R. Belda, *J. Solution Chem.*, 2006, **35**, 1315-1328.
50. E. J. Wensink, A. C. Hoffmann, P. J. van Maaren and D. van der Spoel, *The Journal of chemical physics*, 2003, **119**, 7308-7317.
51. G. Akerlof, *J. Am. Chem. Soc.*, 1932, **54**, 4125-4139.
52. J. Ilavsky and P. R. Jemian, *J. Appl. Crystallogr.*, 2009, **42**, 347-353.
53. J. S. Pedersen, *J. Appl. Crystallogr.*, 2000, **33**, 637-640.
54. V. Cunningham, S. Armes and O. Musa, *Polymer chemistry*, 2016, **7**, 1882-1891.
55. X. Zhang, J. Rieger and B. Charleux, *Polymer Chemistry*, 2012, **3**, 1502-1509.
56. J. Raula, H. Eerikäinen and E. I. Kauppinen, *Int. J. Pharm.*, 2004, **284**, 13-21.
57. E. Jones, M. Semsarilar, P. Wyman, M. Boerakker and S. Armes, *Polymer Chemistry*, 2016, **7**, 851-859.
58. E. Pedraza and M. Soucek, *Polymer*, 2005, **46**, 11174-11185.
59. F. S. Bates and G. H. Fredrickson, *Annu. Rev. Phys. Chem.*, 1990, **41**, 525-557.
60. S. Förster, M. Zisenis, E. Wenz and M. Antonietti, *The Journal of chemical physics*, 1996, **104**, 9956-9970.
61. M. W. Matsen and F. S. Bates, *Macromolecules*, 1996, **29**, 1091-1098.
62. L. A. Fielding, C. T. Hendley IV, E. Asenath-Smith, L. A. Estroff and S. P. Armes, *Polymer Chemistry*, 2019, **10**, 5131-5141.
63. L. Zhang and A. Eisenberg, *J. Am. Chem. Soc.*, 1996, **118**, 3168-3181.
64. M. J. Derry, L. A. Fielding, N. J. Warren, C. J. Mable, A. J. Smith, O. O. Mykhaylyk and S. P. Armes, *Chemical science*, 2016, **7**, 5078-5090.
65. Y. Yu and A. Eisenberg, *J. Am. Chem. Soc.*, 1997, **119**, 8383-8384.
66. E. Jones, O. Mykhaylyk, M. Semsarilar, M. Boerakker, P. Wyman and S. Armes, *Macromolecules*, 2016, **49**, 172-181.
67. Y. Y. Kim, M. Semsarilar, J. D. Carloni, K. R. Cho, A. N. Kulak, I. Polishchuk, C. T. Hendley IV, P. J. Smeets, L. A. Fielding and B. Pokroy, *Adv. Funct. Mater.*, 2016, **26**, 1382-1392.

View Article Online DOI: 10.1039/C9PY01912J

View Article Online
DOI: 10.1039/C9PY01912J

Table of Contents Entry for:

Investigating the Influence of Solvent Quality on RAFT-mediated PISA of Sulfonate-functional Diblock Copolymer Nanoparticles

Shang-Pin Wen, Jack G. Saunders, and Lee A. Fielding*

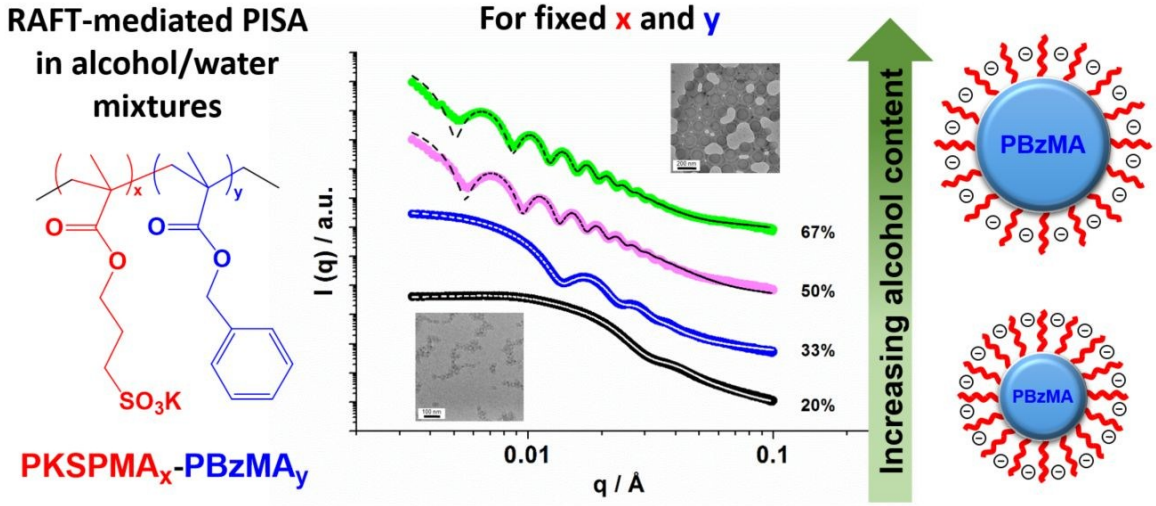

Solvent quality has a marked impact on the assembly of sulfonate-functional diblock copolymer nanoparticles prepared by PISA.